

ARMY RESEARCH LABORATORY



**Quantitative Analysis of Energy and Power on Direct
Methanol Fuel Cell Systems**

by Rongzhong Jiang and Deryn Chu

ARL-TR-3458

April 2005

NOTICES

Disclaimers

The findings in this report are not to be construed as an official Department of the Army position, unless so designated by other authorized documents.

Citation of manufacturers' or trade names does not constitute an official endorsement or approval of the use thereof.

DESTRUCTION NOTICE—Destroy this report when it is no longer needed. Do not return it to the originator.

Army Research Laboratory
Adelphi, MD 20783-1145

ARL-TR-3458

April 2005

**Quantitative Analysis of Energy and Power on Direct
Methanol Fuel Cell Systems**

Rongzhong Jiang and Deryn Chu
Sensors and Electron Devices Directorate, ARL

Approved for public release; distribution unlimited.

REPORT DOCUMENTATION PAGE			Form Approved OMB No. 0704-0188		
Public reporting burden for this collection of information is estimated to average 1 hour per response, including the time for reviewing instructions, searching existing data sources, gathering and maintaining the data needed, and completing and reviewing the collection information. Send comments regarding this burden estimate or any other aspect of this collection of information, including suggestions for reducing the burden, to Department of Defense, Washington Headquarters Services, Directorate for Information Operations and Reports (0704-0188), 1215 Jefferson Davis Highway, Suite 1204, Arlington, VA 22202-4302. Respondents should be aware that notwithstanding any other provision of law, no person shall be subject to any penalty for failing to comply with a collection of information if it does not display a currently valid OMB control number. PLEASE DO NOT RETURN YOUR FORM TO THE ABOVE ADDRESS.					
1. REPORT DATE (DD-MM-YYYY) April 2005		2. REPORT TYPE Progress		3. DATES COVERED (From - To) 10/04-9/05	
4. TITLE AND SUBTITLE Quantitative Analysis of Energy and Power on Direct Methanol Fuel Cell Systems			5a. CONTRACT NUMBER		
			5b. GRANT NUMBER		
			5c. PROGRAM ELEMENT NUMBER		
6. AUTHOR(S) Rongzhong Jiang and Deryn Chu			5d. PROJECT NUMBER		
			5e. TASK NUMBER		
			5f. WORK UNIT NUMBER		
7. PERFORMING ORGANIZATION NAME(S) AND ADDRESS(ES) U.S. Army Research Laboratory Sensors & Electron Devices Directorate (ATTN: AMSRD-ARL-SE-SE) mwellman@arl.army.mil Adelphi, MD 20783-1145			8. PERFORMING ORGANIZATION REPORT NUMBER ARL-TR-3458		
9. SPONSORING/MONITORING AGENCY NAME(S) AND ADDRESS(ES) ARL 2800 Powder Mill Road Adelphi, MD 20783-1145			10. SPONSOR/MONITOR'S ACRONYM(S)		
			11. SPONSOR/MONITOR'S REPORT NUMBER(S)		
12. DISTRIBUTION/AVAILABILITY STATEMENT Approved for public release; distribution unlimited.					
13. SUPPLEMENTARY NOTES					
14. ABSTRACT Two commercial direct methanol fuel cell (DMFC) systems, designed with the same power (25W) but different sizes (size ratio in 11 to 1), were evaluated by constant current discharge at various current loadings and environmental temperatures. Quantitative analysis of fuel consumption and energy output was achieved by a simple mathematical treatment of the experimental data. The larger DMFC system gives higher energy density (770 Wh/Kg) than that of the smaller one (450 Wh/Kg) based on the fuel weight. The smaller DMFC system has higher power density (15.3 W/Kg) than that of the larger one (3.5 W/Kg) based on system weight. Heat dissipation is attributed to be the main problem of limiting the discharge performance for the smaller DMFC system. Too high and too low ambient temperature will cause the energy density to decrease for the DMFC systems. The desire ambient temperature for the present DMFC systems is 20-30 °C. The length of operation time for the DMFC systems also affects the energy output. Minimum time (varying with experimental conditions) is needed for the DMFC system to reach a maximum power and energy output.					
15. SUBJECT TERMS DMFC, Fuel Cell, Fuel Cell System, Energy Analysis					
16. SECURITY CLASSIFICATION OF:			17. LIMITATION OF ABSTRACT UNCLASSIFIED	18. NUMBER OF PAGES 30	19a. NAME OF RESPONSIBLE PERSON Rongzhong Jiang
a. REPORT UNCLASSIFIED	b. ABSTRACT UNCLASSIFIED	c. THIS PAGE UNCLASSIFIED			19b. TELEPHONE NUMBER (Include area code) (301) 394-0295

Standard Form 298 (Rev. 8/98)

Contents

Introduction	1
Experimental	1
DMFC Systems	1
Instrumental and Procedures	2
Results and Discussion	2
Voltage-Current and Power-Current Curves	2
Long Term Discharge Behavior under Constant Current	4
Quantitative Analysis of Energy and Power	10
Conclusion	20
References	21
Distribution list	23

Figures

Figure 1A. Discharge voltage-current and power-current curves of SFC-A25 DMFC system at room temperature (19 ± 1 °C). Cool condition: tested after start up. Warm condition: tested after 1.5A running for 4 hours.	3
Figure 1B. Discharge voltage-current and power-current curves of SFC-C25 DMFC system at different environmental temperatures.	4
Figure 2A. SFC-A25 DMFC performance under constant current discharge (2.0A) at room temperature (19 ± 1 °C).....	5
Figure 2B. Discharge performance of SFC-C25 DMFC system under constant current (2.0A) discharge at room temperature (19 ± 1 °C).	6
Figure 3A. SFC-A25 DMFC performance at high current (4.0A) and room temperature (19 ± 1 °C).	7
Figure 3B. Discharge performance of SFC-C25 DMFC system at high current (2.3A) and room temperature (19 ± 1 °C).	8

Figure 4. Discharge performance of SFC-C25 DMFC system under constant current (2.0A) discharge at high temperature (40 °C).....	9
Figure 5A. Variations of energy density and power with time for SFC-A25 DMFC system under constant current discharge (2.0A).....	12
Figure 5B. Variation of discharge energy density and power with time for SFC-C25 DMFC system under constant current discharge (2.0A) at room temperature (19 ± 1 °C).....	13
Figure 6A. Effect of discharge current on energy density for SFC-A25 DMFC system under constant current discharge at room temperature (19 ± 1 °C).....	14
Figure 6B. Effect of discharge current on energy density for SFC-C25 DMFC system under constant current discharge at room temperature (19 ± 1 °C).....	15
Figure 7A. Effect of discharge current on power output for SFC-A25 DMFC system under constant current discharge at room temperature (19 ± 1 °C).....	16
Figure 7B. Effect of discharge current on power output for SFC-C25 DMFC system at room temperature (19 ± 1 °C).....	17
Figure 8. Effect of environmental temperature on discharge energy density for SFC-C25 DMFC system under constant current (2.0A) discharge.....	18
Figure 9. Effect of environmental temperature on discharge power for SFC-C25 fuel cell system under constant current (2.0A) discharge.....	19

Tables

Table 1. Summary of SFC-A25 DMFC system discharge performance at room temperature (19 ± 1 °C).....	9
Table 2. Summary of SFC-C25 DMFC system discharge performance at room temperature (19 ± 1 °C).....	9
Table 3. SFC-C25 discharge performance under constant current discharge (2.0A) at various environmental temperatures.....	10
Table 4. Effect of discharge current on fuel cartridge utilization at room temperature (19 ± 1 °C).....	13
Table 5. Effect of environmental temperature on fuel cartridge utilization under constant current discharge (2.0A).....	13
Table 6. Summary of SFC-A25 DMFC system performance.....	19
Table 7. Summary of SFC-C25 DMFC system Performance.....	20

Introduction

Portable electric power source plays increasingly important role in communication, portable computers, digital cameras and modern military applications in the 21st century. The available battery technology does not meet the power requirement for these applications. Fuel cell technology is pursued to solve the problem of the need for electric powers. The most promising alternative for battery is direct methanol fuel cell (DMFC) [1-14], which is a type of polymer electrolyte membrane fuel cells. The advantage of DMFC over a hydrogen fuel cell is the high theoretical energy density of methanol (6100 Wh/Kg, base on pure methanol) and the ease of containerization and transportation of liquid fuel. In recent years, the research and development of DMFC has attracted much attention. A practical power source of fuel cells is usually composed of a number of single fuel cells. Such a combination of single fuel cells is called fuel cell stack, which provides higher voltage, current, or power than a single fuel cell. An integration of multiple parts into a power source, such as fuel cell stack, air pumps, fuel pumps, flow meters, heat dissipation fans, transformers, sensors, electric circuit, and start-up-batteries is called as fuel cell system, which can continuously provide electric power as long as fuel is supplied. Several DMFC systems have been demonstrated with different sizes, shapes, materials, and power ranges. Although these DMFC systems are examined when they are made, no report quantitatively analyzing the fuel consumption and energy output for a DMFC system exists. The present article is to compares the effect of design features (compact design and non-compact design) of DMFC system on energy and power output.

Experimental

DMFC Systems

Two DMFC systems were purchased from Smart Fuel Cell AG. One is SFC-A25. The output power by design is 25W. The discharge voltage ranges from 11 to 14V, depending on the output power. The total system volume is 20.4 liter, which is a non-compact design. The fuel cartridge is 2.5 liter, using concentrated methanol as fuel. The air is supplied to the fuel cell by an air-pump. Another DMFC system is SFC-C25. The nominal power by design is 25W. The nominal discharge voltage is 11 V. The total system volume is 1.9 liter, which belongs to a compact design. The fuel cartridge is 125 ml, using 75% methanol as fuel. The air is supplied to the fuel cell by an air-pump. The system volume ratio of the compact to the non-compact DMFC systems is 0.093, although the two systems have about the same power output by design.

Instrumental and Procedures

A battery test station (model No. BT-2043, Arbin Instruments) was used for the electrochemical measurements. The ambient temperature was controlled with a Tenney Environment Chamber (model No. BTRC), which was programmed through a computer with Linktenn II Software. The energy density of the fuel cells was quantitatively determined by constant current discharge. The amount of total fuel consumed was measured by the weighing of the fuel cartridge before and after each discharge experiment.

Results and Discussion

Voltage-Current and Power-Current Curves

The non-compact and compact DMFC systems were generally evaluated by measuring the voltage-current and power-current curves. Figure 1A shows discharge performance of a non-compact DMFC system (SFC-A25). The open circuit voltage of the system is 12V after starting up and 15V after warming up. The voltage-current curves were obtained by multiple consecutive small steps of current change starting from open circuit states. With current going up the voltage goes down until reaching the lower limit of system voltage (10V). The voltage-current curve for the cool condition is relatively straight, which implies an Ohmic-controlled electrochemical behavior. The discharge voltage is significantly higher for the warm condition, and the maximum current can go to 5A before reaching the system voltage limit. The voltage-current curve of the warm condition is relatively bent down, which implies a mass transfer-controlled electrochemical process at the high discharge current range. The power-current curves were obtained by calculation from the voltage-current curves. The maximum discharge power is 31W for the cool condition and 52W for the warm condition. We were unable to measure the effect of environmental temperature on the discharge performance of the non-compact DMFC system because that system's volume was too large to be arranged in the environmental chamber.

Figure 1B shows the discharge performance of a compact DMFC system (SFC-C25). The open circuit voltage decreases from 15V to 13V as environmental temperature increases from 0 to 40 °C. Discharge performance is better the lower the temperature. The compact DMFC system's reverse phenomenon of discharge performance compared to the non-compact system may be attributed to a room too small for sufficient heat dissipation. The maximum discharge power at different environmental temperatures can be found from the power-current curves in the Figure 1B, and they are relatively close with values between 32 – 36W.

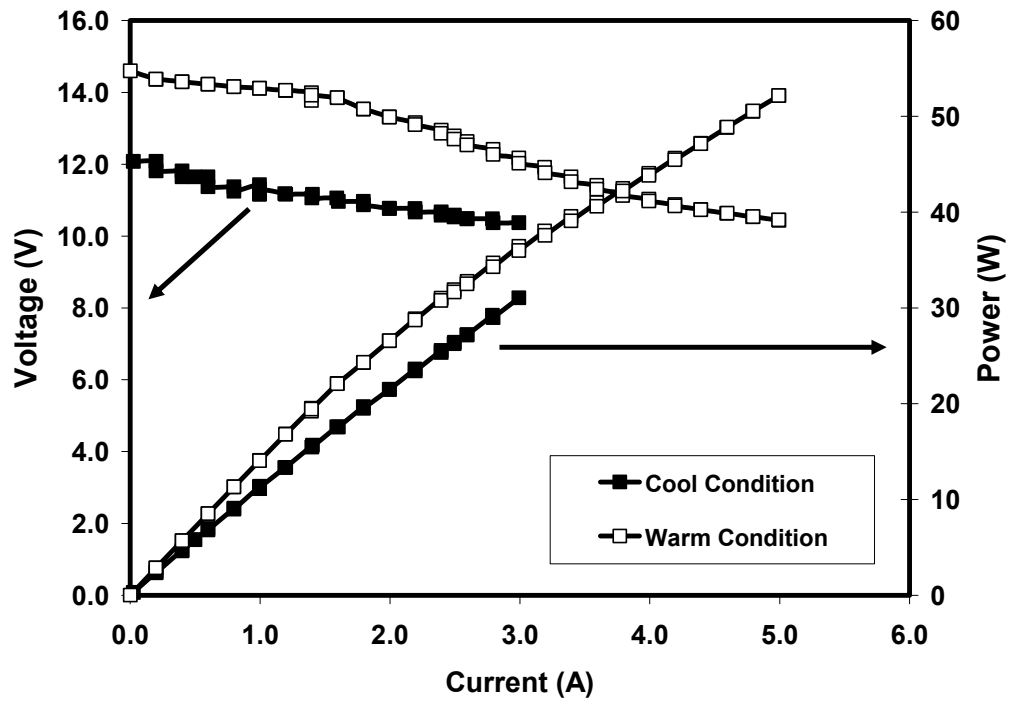


Figure 1A. Discharge voltage-current and power-current curves of SFC-A25 DMFC system at room temperature (19 ± 1 °C). Cool condition: tested after start up. Warm condition: tested after 1.5A running for 4 hours.

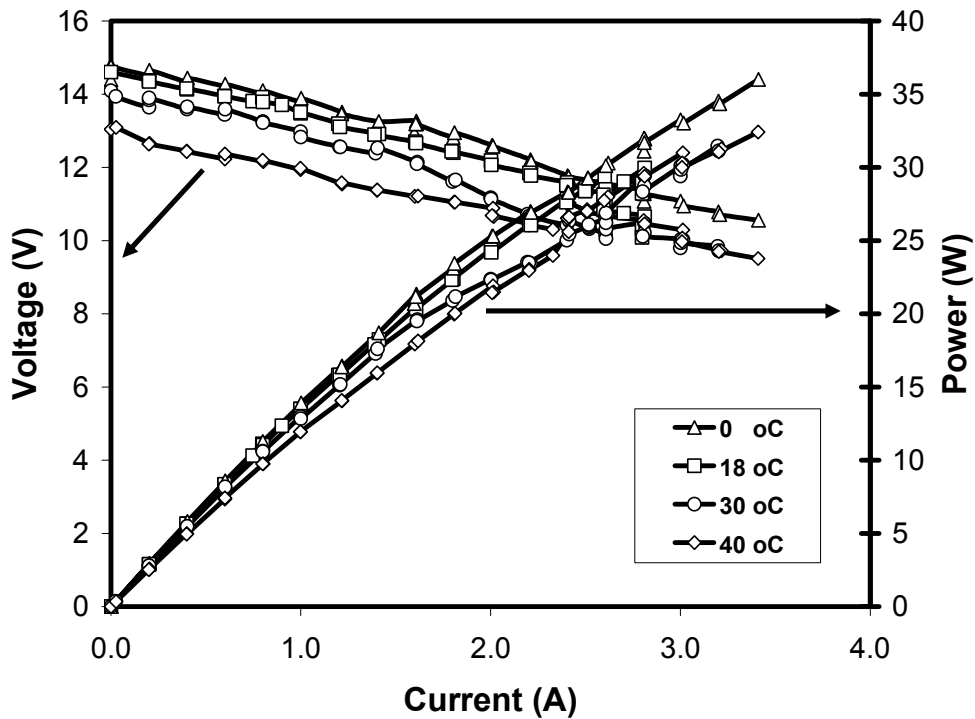


Figure 1B. Discharge voltage-current and power-current curves of SFC-C25 DMFC system at different environmental temperatures.

Long Term Discharge Behavior under Constant Current

A voltage-current curve describes only the short term behavior of a DMFC system. In general, the long term behavior of a DMFC system is different than the short term behavior due to system factor changes in heat dissipation and mass transfer. Constant current discharge is a convenient way to measure a long term discharge performance. Figure 2A shows voltage-time curve of the non-compact DMFC system under constant current discharge (2.0A). Because of periodical air purging in the DMFC system, the voltage-time curve is not smooth, but fluctuates with the same periodical term. The step of purging air is designed to freshen the air electrode and to increase the performance of the fuel cell. The fluctuation of the voltage-time curve does not affect analyzing the data of the DMFC system if these fluctuated data points are not considered in the data treatment. As shown in Figure 2A, the voltage slowly increases with time, and becomes constant for a few hours later (without considering the fluctuated points). The discharge voltage is 12V at the beginning, and finally reaches 13V. No voltage decrease was found for continuous operation of the DMFC system.

Figure 2B shows voltage-time curve of the compact DMFC system under constant current discharge (2A). Voltage fluctuation is also seen in the figure due to purging air by the internal system design. Therefore, in the present article the fluctuated data points are

not considered. The average discharge voltage of the compact DMFC system is 12V, about 1V lower than that of the non-compact DMFC system.

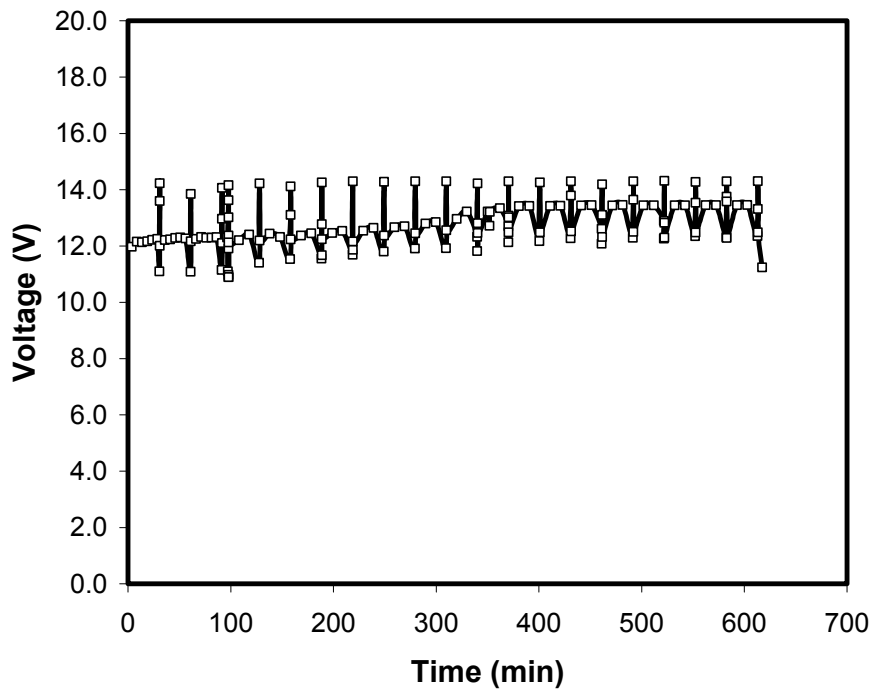


Figure 2A. SFC-A25 DMFC performance under constant current discharge (2.0A) at room temperature (19 ± 1 °C).

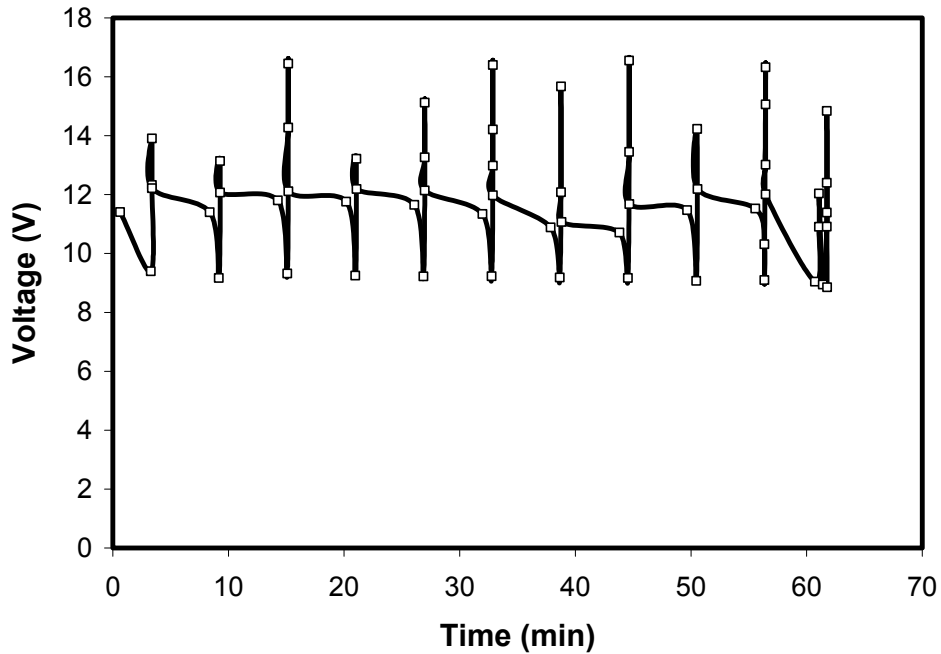


Figure 2B. Discharge performance of SFC-C25 DMFC system under constant current (2.0A) discharge at room temperature (19 ± 1 °C).

Increasing discharge current causes production of more heat, and eventually results in heat dissipation problem. Figure 3A and 3B show voltage-time curves under high current discharge for the non-compact and compact DMFC systems. For the non-compact DMFC system, a maximum current of 4.0A can be applied. For the compact DMFC system, only 2.3A maximum current can be used. Under high current discharge the DMFC systems can operate only less than 20 minutes and must then be turned off due to reaching the system temperature limits. Heat dissipation causing problems with the DMFC system is further confirmed by increasing the environmental temperature. Figure 4 shows voltage-time curves at high environmental temperature under constant current (2.0A) discharge. The maximum operation time under this condition is only 20 minutes.

The effect of discharge current on the operation performance of non-compact and compact DMFC systems is summarized in Table 1 and Table 2, respectively. Increasing discharge current results in decreasing average voltage and increasing average power. The effect of environmental temperature on the performance of compact DMFC system is summarized in Table 3. The variation of environmental temperature seems not to cause significant changes to average voltage and average power.

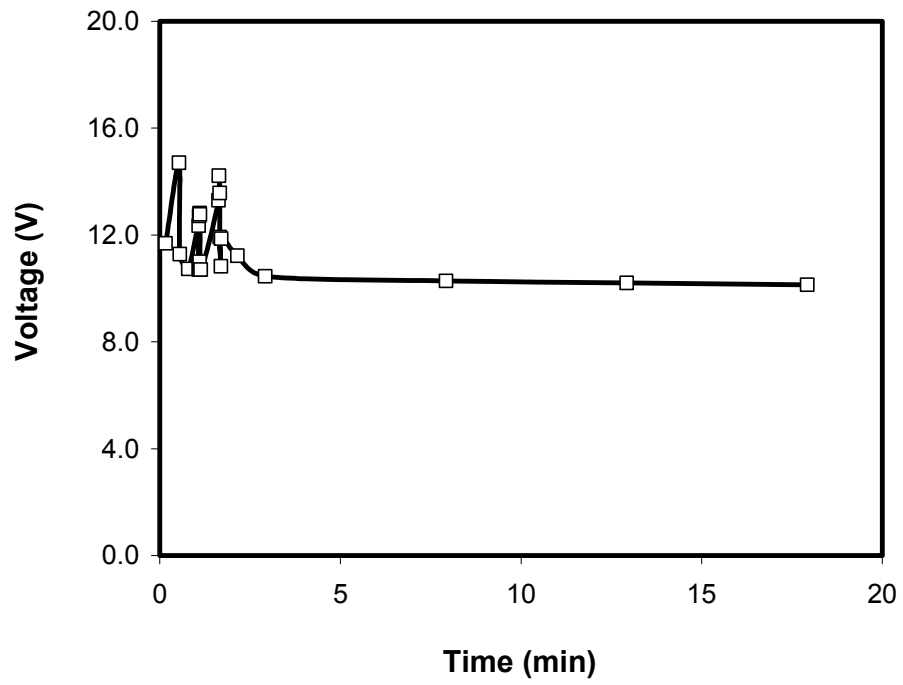


Figure 3A. SFC-A25 DMFC performance at high current (4.0A) and room temperature (19 ± 1 °C).

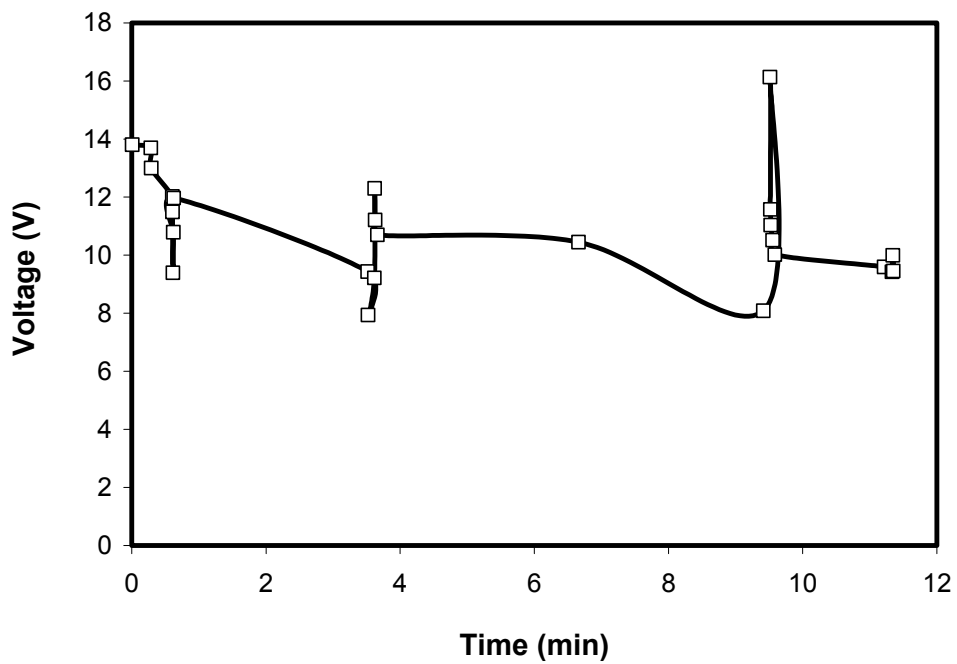


Figure 3B. Discharge performance of SFC-C25 DMFC system at high current (2.3A) and room temperature (19 ± 1 °C).

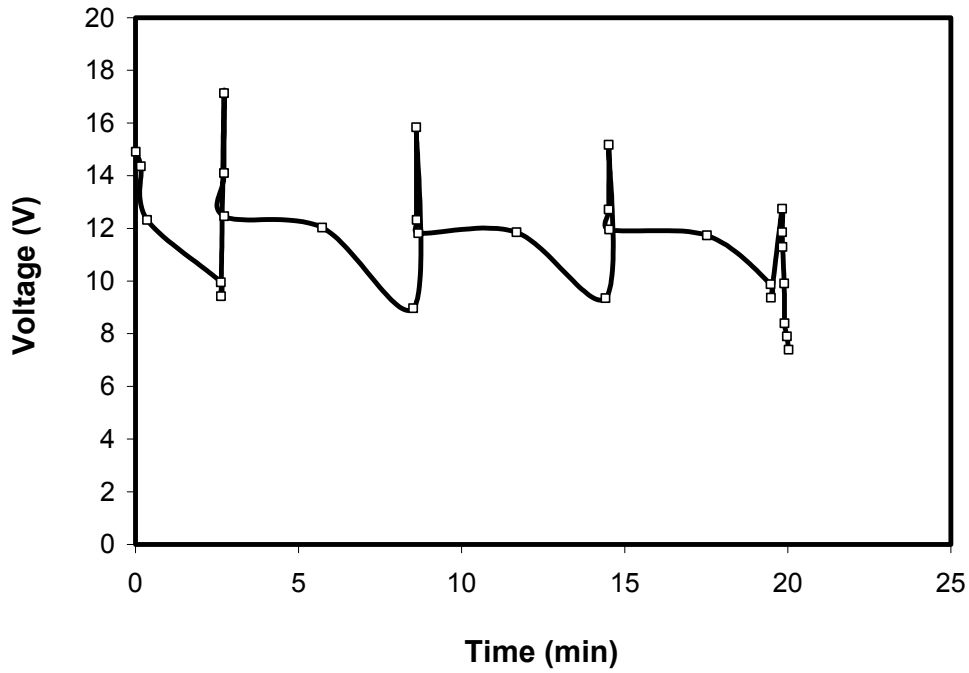


Figure 4. Discharge performance of SFC-C25 DMFC system under constant current (2.0A) discharge at high temperature (40 °C).

Table 1. Summary of SFC-A25 DMFC system discharge performance at room temperature (19 ± 1 °C).

Current (A)	1.5	2.0	3.0	4.0
Average Voltage (V)	14	13	11	10
Average Power (W)	20	26	34	41
Energy Density (Wh/Kg Fuel)	333	722	771	753

Table 2. Summary of SFC-C25 DMFC system discharge performance at room temperature (19 ± 1 °C).

Current (A)	1.5	2.0	2.3
Average Voltage (V)	12.5	11.5	10.0
Average Power (W)	18.8	23.0	23.0
Energy Density (Wh/Kg Fuel)	404.2	456.5	190.8

Table 3. SFC-C25 discharge performance under constant current discharge (2.0A) at various environmental temperatures.

Temperature. (°C)	Average Voltage (V)	Average Power (W)	Energy Based on Fuel (Wh/Kg)
0	11.0	22.0	228.6
18	11.5	23.0	456.5
30	11.0	22.0	496.7
40	11.5	23.0	488.3

Quantitative Analysis of Energy and Power

Generally, quantitative analysis of commercial DMFC systems is difficult because of many unknown factors affecting complex system integration, such as stack configuration, cell numbers in a fuel cell stack, style of air supply, fuel concentration, heat dissipation, operation of startup battery, and internal consumption of energy.

We quantitatively analyze two types of DMFC systems, emphasizing energy output and fuel consumption.

The energy output can be quantitatively calculated from the data of the voltage – time curves shown in Figure 2A and 2B. Here, we describe a method of analyzing energy conversion in the DMFC system under constant current discharge. The output energy can be expressed by an equation,

$$E = \frac{i}{3600} \int_0^t v(t) dt \quad (1)$$

Where, E (energy, Wh) is the output energy of the fuel cell system; i (Ampere, A) is the discharge current; t (Second, s) is the time of the discharge process. v (Voltage, V) is the stack voltage, and $v(t)$ is a function of stack voltage versus time.

According to electrochemical knowledge, the consumed amount of fuel is proportional to the discharge capacity if neglecting the factor of fuel crossover or considering that the lost fuel by crossover is equal for per unit of time. Under constant current discharge the consumed fuel amount is also proportional to the discharge time. Therefore, we have,

$$W = Ct \quad (2)$$

Where, W (g) is the amount of consumed fuel, and C ($\text{g}\cdot\text{s}^{-1}$) is a constant. Therefore, the output energy density E_d ($\text{Wh}\cdot\text{kg}^{-1}$) can be expressed as,

$$E_d = \frac{1000i}{3600Ct} \int_0^t v(t) dt \quad (3)$$

The constant, C , in equation (3) can be obtained from the weight loss of fuel cartridge for a time period during discharge. The function, $v(t)$, is known from the voltage-time curves. Therefore, the equation (3) can be solved, and we can quantitatively describe the energy density for all the discharge time.

Figure 5A shows variations of energy density and discharge power with time for the non-compact DMFC system. The energy density increases sharply from zero at the beginning time, then continues to increase very slowly, eventually reaching a plateau after a long time period. This phenomenon implies that the energy or fuel efficiency is affected by the length of an operation time of the DMFC system. The power-current curve is almost a plateau in Figure 5A, with only a small increase over time. Periodical fluctuation of power is seen in the power-time curve because of purging air by the DMFC system. However, the energy-time curve is smooth and without fluctuation, which indicates that short time purging of air apparently does not affect the integration of energy.

Figure 5B shows variations of energy density and discharge power over time for the compact DMFC system. The energy density and discharge power have similar variations to those in figure 5A. However, the compact DMFC system self stopped for only a short time running due to the fuel limitation. The percentage of fuel cartridge use is summarized in Table 4 and 5. The fuel is unable to be completely used in the fuel cartridge. The highest fuel cartridge use is only 30.5% at room temperature under 2.0A discharge. Increasing current density or increasing temperature will cause fuel cartridge use to decrease due to overheating of the DMFC system.

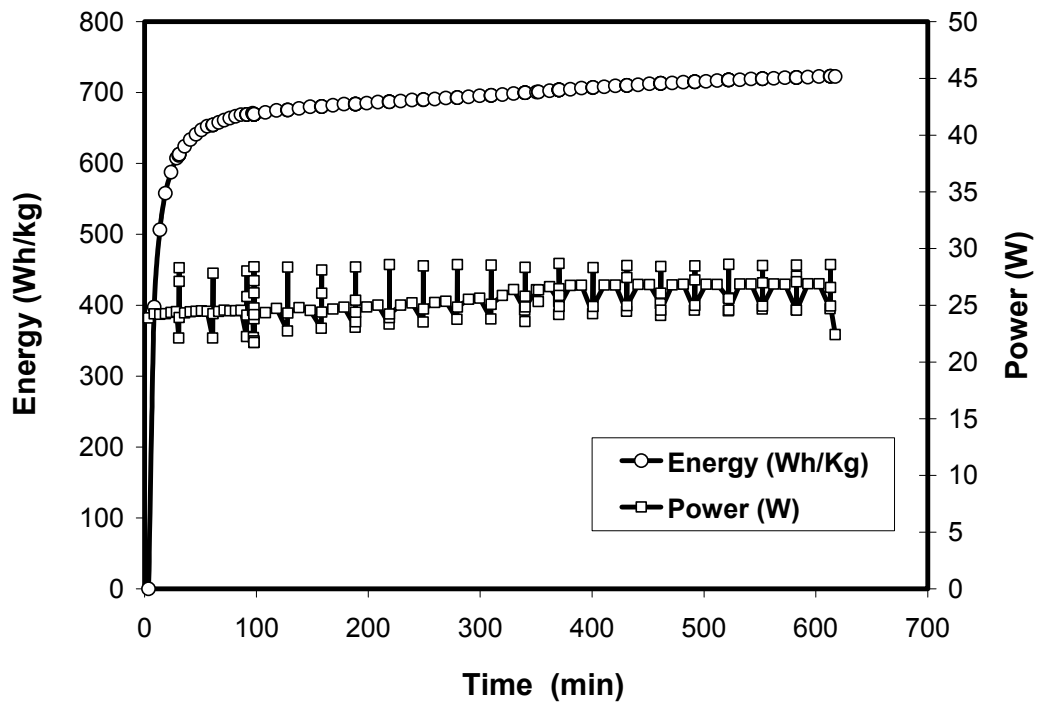


Figure 5A. Variations of energy density and power with time for SFC-A25 DMFC system under constant current discharge (2.0A).

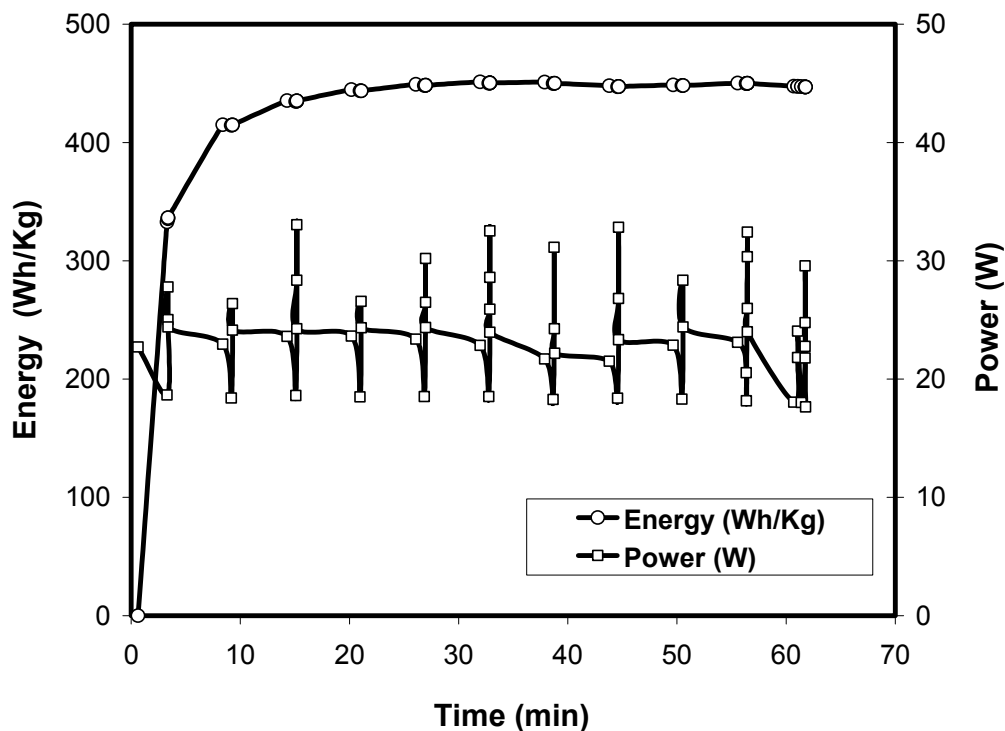


Figure 5B. Variation of discharge energy density and power with time for SFC-C25 DMFC system under constant current discharge (2.0A) at room temperature (19 ± 1 °C).

Table 4. Effect of discharge current on fuel cartridge utilization at room temperature (19 ± 1 °C).

Current (A)	1.5	2.0	2.3
Time Lasted (min)	60.5	61.8	11.3
Fuel Consumed (g)	46.9	51.9	22.7
Fuel Cartridge Utilization (%)	27.6	30.5	13.4

Table 5. Effect of environmental temperature on fuel cartridge utilization under constant current discharge (2.0A).

Temperature °C	0	18	30	40
Time Lasted (min)	27	61.8	52.7	20.0
Fuel Consumed (g)	44.3	51.9	38.9	29.2
Fuel Cartridge Utilization (%)	26.1	30.5	22.9	17.2

Figure 6A shows the effect of discharge current on energy density for the non-compact DMFC system. All these energy-time curves eventually form flat plateaus. Increasing the discharge current from 1.5A to 3.0A the plateau of energy density jumps appreciably. The maximum energy density is about 770 Wh/kg (based on fuel) for current 3.0A. The average energy density under different current discharge for the non-compact DMFC system is listed in Table 1.

Figure 6B shows the effect of discharge current on energy density for the compact DMFC system. Increasing discharge current from 1.5A to 2.3A increases the energy density. However, the maximum energy density is limited to only about 450 Wh/kg for current 2.0A. The poor performance of 2.3A discharge is attributed to system overheat. The average energy density under different current discharge for the compact DMFC system is listed in Table 2.

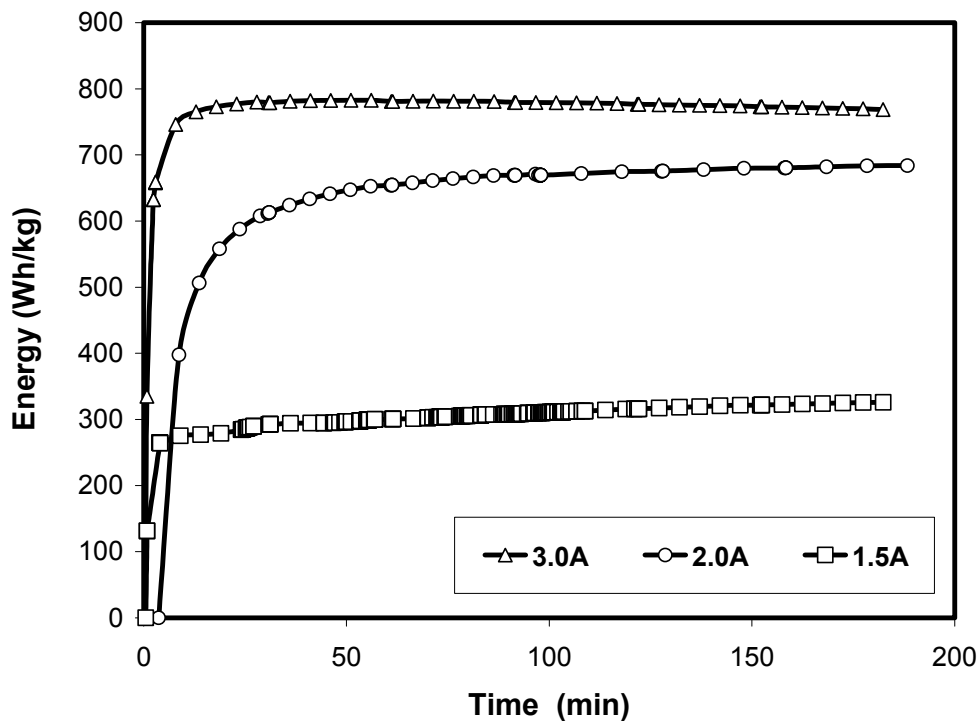


Figure 6A. Effect of discharge current on energy density for SFC-A25 DMFC system under constant current discharge at room temperature (19 ± 1 °C).

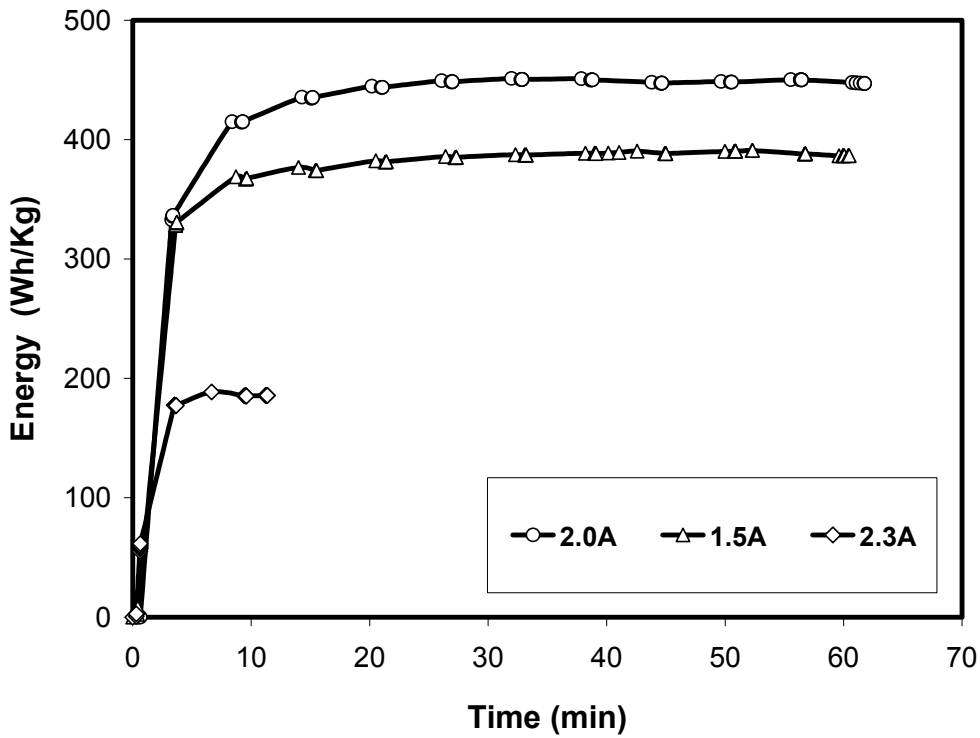


Figure 6B. Effect of discharge current on energy density for SFC-C25 DMFC system under constant current discharge at room temperature (19 ± 1 °C).

Figures 7A and 7B show effect of discharge current on power output for the non-compact and compact DMFC systems respectively. These power-current curves form flat plateaus if not considering the experimental points by purging air. If discharge current is the same, the results of power output are relatively close by comparing the non-compact and compact DMFC systems. The non-compact DMFC system has higher discharge power because it can go to higher discharge current without causing a thermal problem.

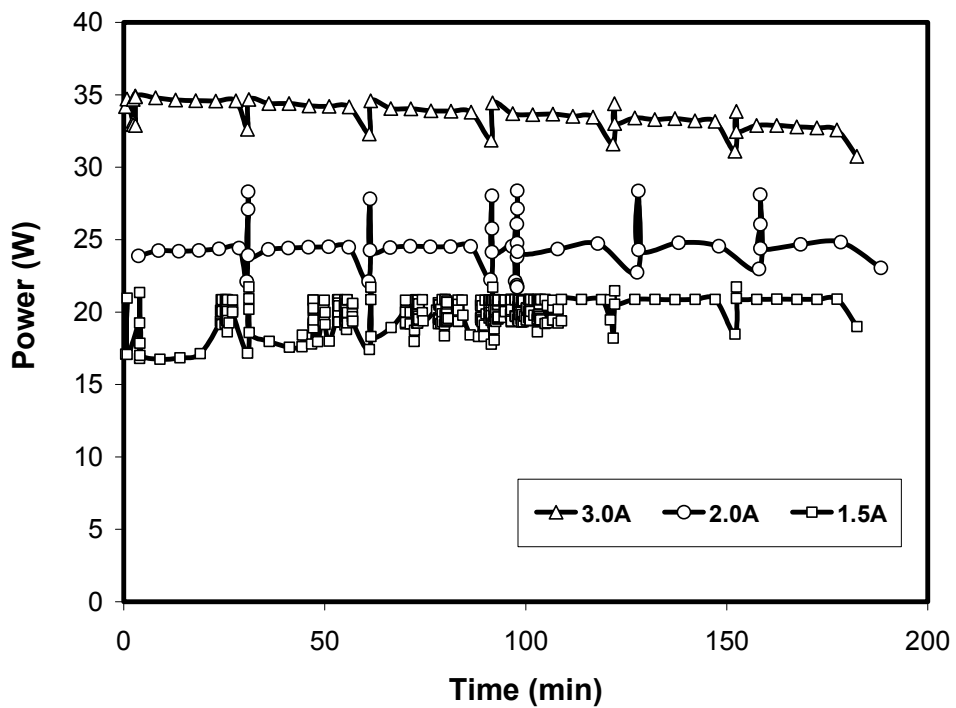


Figure 7A. Effect of discharge current on power output for SFC-A25 DMFCI system under constant current discharge at room temperature (19 ± 1 °C).

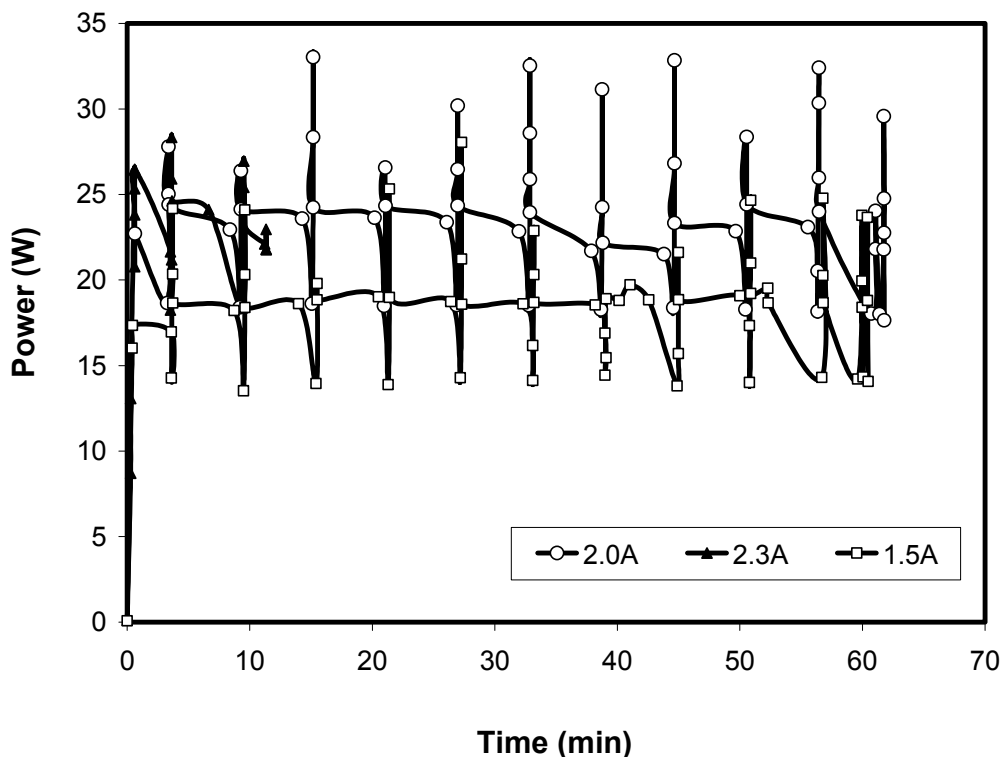


Figure 7B. Effect of discharge current on power output for SFC-C25 DMFC system at room temperature ($19 \pm 1 \text{ }^\circ\text{C}$).

Figure 8 shows effect of environmental temperature on discharge energy density for the compact DMFC system. The highest discharge energy density is obtained at $30 \text{ }^\circ\text{C}$. Increasing or decreasing temperature will cause energy density to decrease, and result in a self stopping of the DMFC system in a short operation time. The reason for the energy density drop is heat loss and lower electrochemical kinetics of the DMFC system in low temperature. Figure 9 shows the power output at various temperatures for the compact DMFC system. The power output variation is not appreciable ($22 - 23 \text{ W}$) at different temperatures. Table 3 summarizes energy density and power output for the compact DMFC system at different temperatures. The overall discharge performance and electrochemical data for the non-compact and compact DMFC systems are summarized in Table 6 and Table 7 respectively.

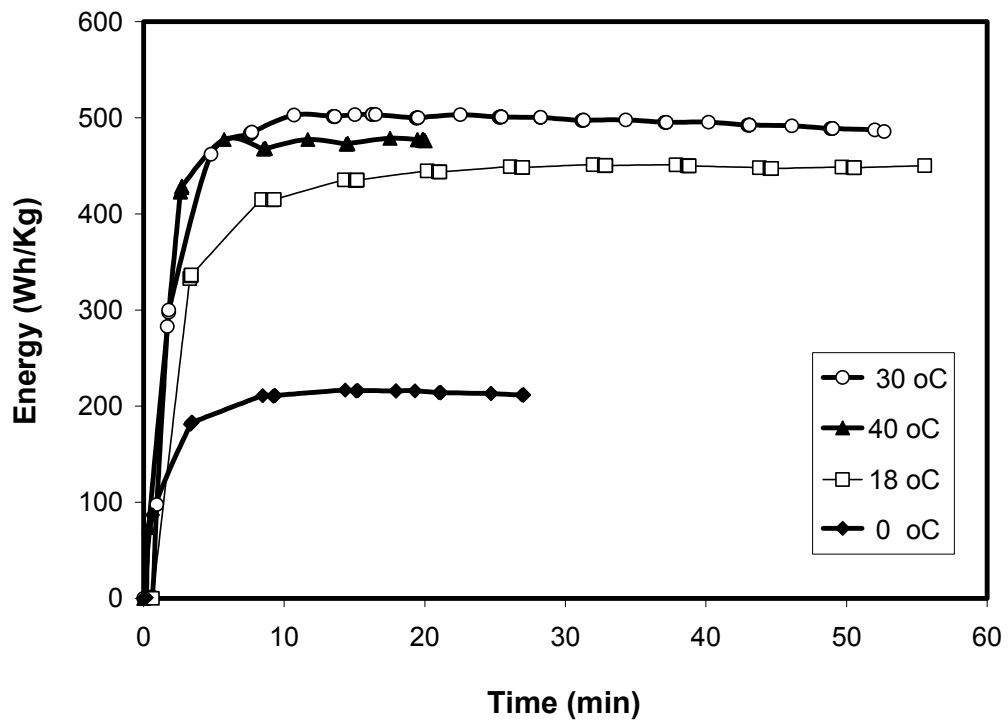


Figure 8. Effect of environmental temperature on discharge energy density for SFC-C25 DMFC system under constant current (2.0A) discharge.

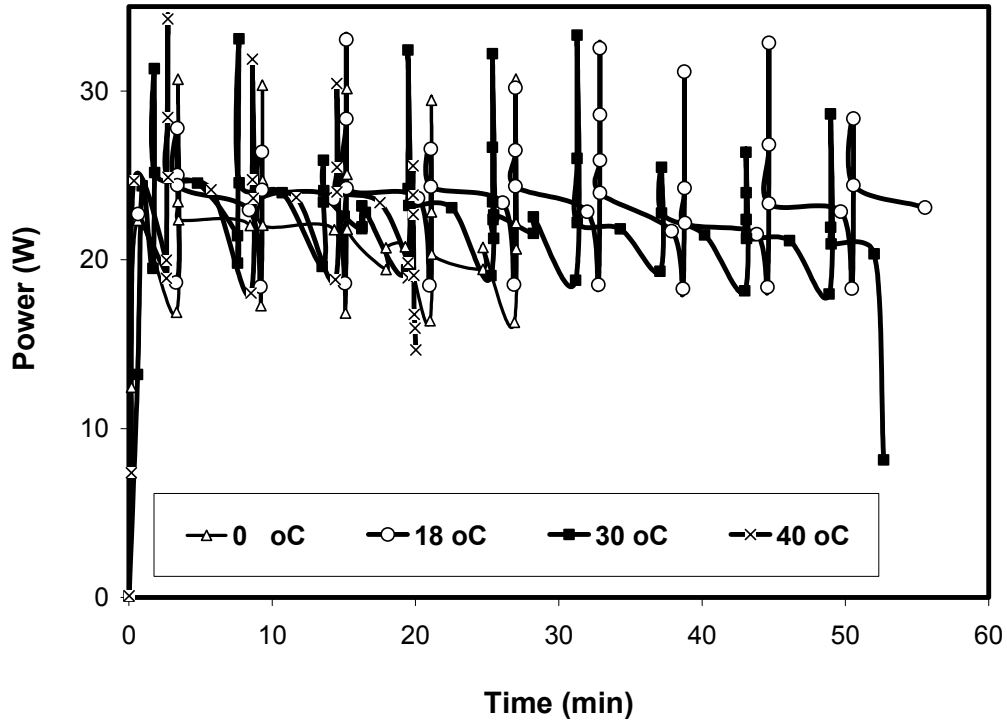


Figure 9. Effect of environmental temperature on discharge power for SFC-C25 fuel cell system under constant current (2.0A) discharge.

Table 6. Summary of SFC-A25 DMFC system performance.

System Weight + Fuel Cartridge (Kg)	9.7
Fuel Cartridge Weight (Kg)	2.2
Fuel Cartridge Volume (dm ³)	2.5
System Size (dm ³)	20.4
Average Voltage (V) (at 3A discharge)	11
Average Power (W)*	34
System Power Density (W/Kg)*	3.5
System Power Density (W/L)*	1.7
Energy Based on Fuel (Wh/Kg)*	771
Energy Based on Fuel Cartridge (Wh/Kg)*	701
Time needed for 1 cartridge to be full discharged at 3A (Hour)	46
Energy Based on SFC-A25 System and Fuel Cartridge (Wh/Kg)*	159 for 1 cartridge used

* Calculated with the data at 3A discharge.

Table 7. Summary of SFC-C25 DMFC system Performance.

System Weight (Kg)	1.5
Fuel Cartridge Weight (g)	170
System Size (cm ³)	1939.2 (19.4 x 12.25 x 8.16)
Average Voltage (V)	11.5
Average Power (W)	23
System Power Density (W/Kg)	15.3
System Power Density (W/L)	11.9
Energy Base on Fuel (Wh/Kg)	450
Energy Based on Fuel Cartridge (Wh/Kg)*	159
Energy Based on SFC-C25 System and Fuel Cartridge (Wh/Kg)**	16 (for 1 cartridge used)

* About 60g methanol can be utilized for one fuel cartridge.

** The total weight of system and fuel cartridge is 1.67Kg.

Conclusion

Quantitative analysis of energy density and fuel consumption for DMFC systems can be achieved under constant current discharge with a sample mathematical treatment of experimental data. By comparing two DMFC systems with non-compact and compact designs, the non-compact system has better heat dissipation and higher energy density based on fuel weight. The compact system has higher power density based on system weight.

References

1. S. Surampudi, S. R. Narayanan, E. Vamos, H. Frank, G. Halpert, A. Laconti, J. Kosek, G. K. S. Prakash, and G. A. Olah, *J. Power Sources*, 47, 377 (1994). "Advances in direct oxidation methanol Fuel cells."
2. X. M. Ren, M. S. Wilson, and S. Gottesfeld, *J. Electrochem. Soc.*, 143, L12 (1996). "High performance direct methanol polymer electrolyte fuel cells."
3. Q. B. Fan, C. Pu and E. S. Smotkin, *J. Electrochem. Soc.*, 143, 3053 (1996). "Ins situ Fourier transform infrared-diffuse reflection spectroscopy of direct methanol fuel cell anodes and cathodes."
4. D. Chu and S. Gilman, *J. Electrochem. Soc.*, 143, 1685 (1996). "Methanol electro-oxidation on unsupported Pt-Ru alloys at different temperatures."
5. J. T. Wang, J. S. Wainright, R. F. Savinell and M. Litt, *J. Applied Electrochem.*, 26, 751 (1996). "A direct methanol fuel cell using acid-doped polybenzimidazole as polymer electrolyte."
6. C. K. Witham, W. Chun, T. I. Valdez, S. R. Narayanan, *Electrochemical and Solid State Letters*, 3, 497 (2000). "Performance of direct methanol fuel cell with sputter-deposited anode catalyst layers."
7. X. M. Ren, P. Zelenay, S. Thomas, J. Davey and S. Gottesfeld, *J. Power Sources*, 86, 111 (2000). "Recent advances in direct methanol fuel cells at Los Alamos National Laboratory."
8. A. S. Arico, S. Srinivasan and A. Antonucci, *Fuel cells*, 1, 133 (2001). "DMFCs: From Fundamental Aspects to Technology Development."
9. D. Chu and S. Gilman, *J. Electrochem. Soc.*, 141, 1770 (1994). "The Influence Of Methanol On O₂ Electroreduction At A Rotating Pt Disk Electrode In Acid Electrolyte."
10. R. Jiang and D. Chu, *J. Electrochem. Soc.*, 147, 4605 (2000). "Remarkably active catalysts for the electroreduction of O₂ to H₂O for use in an acidic electrolyte containing concentrated methanol."
11. X. M. Ren, T. E. Springer, T. A. Zawodzinski and S. Gottesfeld, *J. Electrochem. Soc.*, 147, 466 (2000). "Methanol transports through Nafion membranes, electro-osmotic drag effects on potential step measurements."

12. Rongzhong Jiang and Deryn Chu, *Electrochem. Solid-State Lett.*, 5 (7), A156-A159 (2002). "CO₂ Crossover through A Nafion Membrane in A Direct Methanol Fuel Cell."
13. Rongzhong Jiang, Charles Rong and Deryn Chu, *Journal of Power Sources*, 126, 119-124, (2004). "Determination of energy efficiency for a direct methanol fuel cell stack by a method of fuel circulation."
14. Rongzhong Jiang and Deryn Chu, *Journal of the Electrochemical Society*, 151, A69-A76, (2004). "Comparative Studies of Methanol Crossover and Cell Performance for a Direct Methanol Fuel Cell."

Distribution list

Admnstr
Defns Techl Info Ctr
ATTN DTIC-OCP (Electronic copy)
8725 John J Kingman Rd Ste 0944
FT Belvoir VA 22060-6218

DARPA
Ofc of the Secy of Defns
ATTN IXO S Welby
ATTN ODDRE (R&AT)
The Pentagon
Washington DC 20301-3080

CECOM NVESD
ATTN AMSEL-RD-NV-D
FT Belvoir VA 22060-5806

Commander
CECOM R&D
ATTN AMSEL-IM-BM-I-L R Hamlen
ATTN AMSEL-IM-BM-I-L-R Stinfo
Ofc
ATTN AMSEL-IM-BM-I-L-R Techl
Lib
FT Monmouth NJ 07703-5703

SMC/GPA
2420 Vela Way Ste 1866
El Segundo CA 90245-4659

Commanding General
US Army Avn & Mis Cmnd
ATTN AMSAM-RD W C McCorkle
Redstone Arsenal AL 35898-5000

Commander
US Army CECOM
ATTN AMSEL-RD-CZ-PS-B M
Brundage
FT Monmouth NJ 07703-5000

Commander
US Army CECOM RDEC
ATTN AMSEL-RD-AS-BE E Plichta
FT Monmouth NJ 07703-5703

US Army Info Sys Engrg Cmnd
ATTN SCBRD-TD G Resnick
ATTN AMSEL-IE-TD F Jenia
FT Huachuca AZ 85613-5300

US Army Natick RDEC
Acting Techl Dir
ATTN SBCN-TP P Brandler
Kansas Street Bldg 78
Natick MA 01760-5056

Nav Rsrch Lab
ATTN Code 2627
Washington DC 20375-5000

USAF Rome Lab Tech
ATTN Corridor W Ste 262 RL SUL
26 Electr Pkwy Bldg 106
Griffiss AFB NY 13441-4514

Hicks & Assoc Inc
ATTN G Singley III
1710 Goodrich Dr Ste 1300
McLean VA 22102

Palisades Inst for Rsrch Svc Inc
ATTN E Carr
ATTN Documents
1745 Jefferson Davis Hwy Ste 500
Arlington VA 22202-3402

Director
US Army Rsrch Lab
ATTN AMSRD-ARL-RO-D JCI
Chang
ATTN AMSRL-RO-EN B Mann
PO Box 12211
Research Triangle Park NC 27709-2211

US Army Rsrch Lab
ATTN AMSRD-ARL-CI-OK-T Techl
Pub (2 copies)
ATTN AMSRD-ARL-CI-OK-TL Techl
Lib (2 copies)
ATTN AMSRD-ARL-D J M Miller
ATTN AMSRD-ARL-SE J Pellegrino
ATTN AMSRD-ARL-SE-D E
Scannell
ATTN AMSRD-ARL-SE-E J Mait
ATTN AMSRL-RO-PS R Paur
ATTN AMSRL-SE-DC D Chu (5
copies)
ATTN AMSRL-SE-DC R Jiang (5
copies)
ATTN AMSRL-SE-DC S Gilman
ATTN IMNE-ALC-IMS Mail &
Records Mgmt